Article

Cell Reports

Increased Airway Reactivity and Hyperinsulinemia in Obese Mice Are Linked by ERK Signaling in Brain Stem Cholinergic Neurons

Graphical Abstract

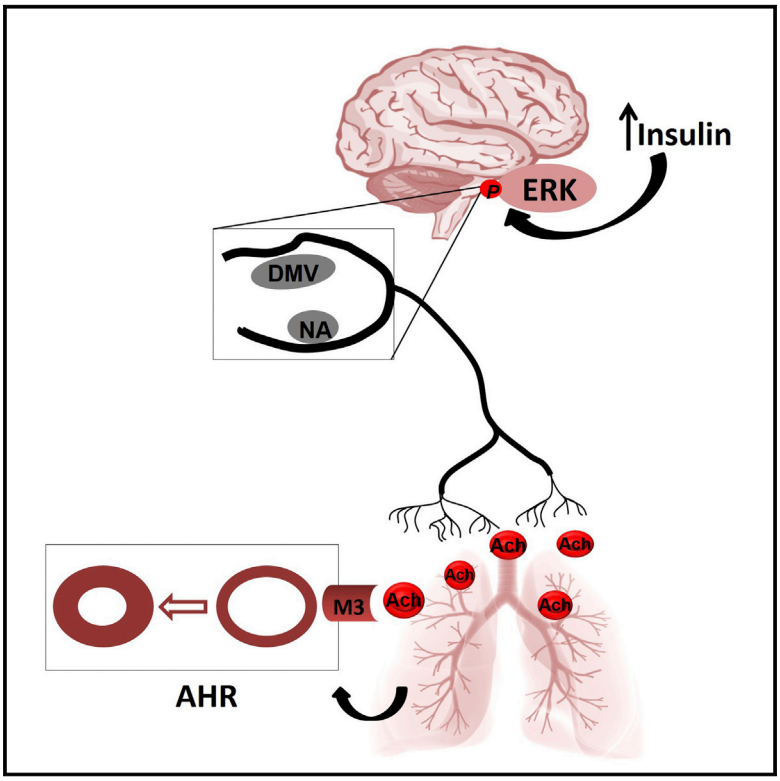

Highlights

- Excess circulating insulin causes airway hyperreactivity in obese mice
- This relies on activation of cholinergic nerves in the brain stem
- Activation of ERK in these neurons is required for obesity-related airway hyperreactivity

Authors

Luiz O.S. Leiria,
Fernanda M. Arantes-Costa, ...,
Milton A. Martins, Mario J.A. Saad

Correspondence

msaad@fcm.unicamp.br

In Brief

Obesity and hyperinsulinemia are risk factors for asthma, but the mechanisms underlying this association have not been elucidated. Leiria et al. demonstrate that increased levels of insulin trigger a signaling pathway through cholinergic neurons in the brain stem that can increase airway reactivity in obese mice.

Leiria et al., 2015, Cell Reports *11*, 934–943
May 12, 2015
http://dx.doi.org/10.1016/j.celrep.2015.04.012

CellPress

OPEN ACCESS
CellPress

Cell Reports
Article

Increased Airway Reactivity and Hyperinsulinemia in Obese Mice Are Linked by ERK Signaling in Brain Stem Cholinergic Neurons

Luiz O.S. Leiria,[1] Fernanda M. Arantes-Costa,[2] Marina C. Calixto,[3] Eduardo C. Alexandre,[3] Rodrigo F. Moura,[1,4] Franco Folli,[1,4,5] Carla M. Prado,[6] Marco Antonio Prado,[7] Vania F. Prado,[7] Licio A. Velloso,[1,4] José Donato, Jr.,[8] Edson Antunes,[3] Milton A. Martins,[2] and Mario J.A. Saad[1,4,*]

[1]Department of Internal Medicine, Faculty of Medical Sciences, State University of Campinas, Campinas, SP 13083-887, Brazil
[2]Department of Medicine, School of Medicine, University of São Paulo, São Paulo, SP 01246-904, Brazil
[3]Department of Pharmacology, Faculty of Medical Sciences, State University of Campinas, Campinas, SP 13083-881, Brazil
[4]Obesity and Comorbidities Research Center (O.C.R.C.), State University of Campinas, Campinas, SP 13083-887, Brazil
[5]Division of Diabetes, Department of Medicine, University of Texas Health Science Center at San Antonio, TX 78229-3900, USA
[6]Department of Biological Science, Federal University of São Paulo, Diadema, SP 09972-270, Brazil
[7]Robarts Research Institute, Department of Anatomy & Cell Biology and Department of Physiology and Pharmacology, University of Western Ontario, London, ON 5015, Canada
[8]Department of Physiology, Institute of Biomedical Sciences, University of São Paulo, São Paulo, SP 05508-000, Brazil
*Correspondence: msaad@fcm.unicamp.br
http://dx.doi.org/10.1016/j.celrep.2015.04.012

SUMMARY

Obesity is a major risk factor for asthma, which is characterized by airway hyperreactivity (AHR). In obesity-associated asthma, AHR may be regulated by non-T_H2 mechanisms. We hypothesized that airway reactivity is regulated by insulin in the CNS, and that the high levels of insulin associated with obesity contribute to AHR. We found that intracerebroventricular (ICV)-injected insulin increases airway reactivity in wild-type, but not in vesicle acetylcholine transporter knockdown (VAChT $KD^{HOM-/-}$), mice. Either neutralization of central insulin or inhibition of extracellular signal-regulated kinases (ERK) normalized airway reactivity in hyperinsulinemic obese mice. These effects were mediated by insulin in cholinergic nerves located at the dorsal motor nucleus of the vagus (DMV) and nucleus ambiguus (NA), which convey parasympathetic outflow to the lungs. We propose that increased insulin-induced activation of ERK in parasympathetic pre-ganglionic nerves contributes to AHR in obese mice, suggesting a drug-treatable link between obesity and asthma.

INTRODUCTION

Recent studies have provided clinical and experimental evidence for a common association between obesity and asthma (Al-Alwan et al., 2014; Dixon et al., 2011; Sideleva et al., 2012; Wenzel, 2012). In the most common asthma phenotypes, allergic asthma accompanied by pulmonary eosinophilic infiltration is regarded as the major cause of bronchoconstriction. On the other hand, obesity-associated asthma is not always accompanied by the classic T-helper 2 (T_H2) inflammation in the bronchial walls, and affected subjects are often resistant to first-line glucocorticoid drugs (Leiria et al., 2015; Peters-Golden et al., 2006). Thus, a T_H2-independent mechanism is likely to contribute to airway hyperreactivity (AHR) in obesity.

An emerging line of clinical and epidemiological investigation has proposed a positive correlation between hyperinsulinemia and asthma independent of the body mass index (Arshi et al., 2010; Husemoen et al., 2008; Thuesen et al., 2009). Accordingly, in the context of the pathophysiology of obesity-related asthma, hyperinsulinemia and insulin resistance would not be only predictors, but also risk factors for asthma in children and adults (Husemoen et al., 2008; Thuesen et al., 2009). Interestingly, a recent study has shown that central leptin (an important hormone involved in the pathogenesis of obesity/diabetes) is capable of increasing the airways' diameter via a negative regulation of the airway-related pre-ganglionic parasympathetic fibers (ARPFs) (Arteaga-Solis et al., 2013). Moreover, under extreme body weight condition, leptin resistance was reported to contribute to AHR in high-fat-fed obese mice, suggesting that a neuroendocrine mechanism is capable of regulating AHR under obesity condition (Arteaga-Solis et al., 2013).

Cholinergic ARPF arises primarily from the rostral nucleus ambiguus (rNA) and to a lesser degree from the dorsal motor nucleus of the vagus (DMV), both of which are located at the brain stem (Fontán et al., 2000; Pérez Fontán and Velloff, 2001). The brain stem ARPFs are the final common pathway from the brain to the lungs, and, once fired, ARPFs transmit signals to the intrinsic tracheobronchial ganglia, which lie in close proximity to the effector tissue (Baker et al., 1986; Dey et al., 1996; Maize et al., 1998). Finally, postganglionic neurons convey the signal up to the airway neuroeffector site, where acetylcholine (ACh) is then released to increase the airway's tonus (Arteaga-Solis et al., 2013).

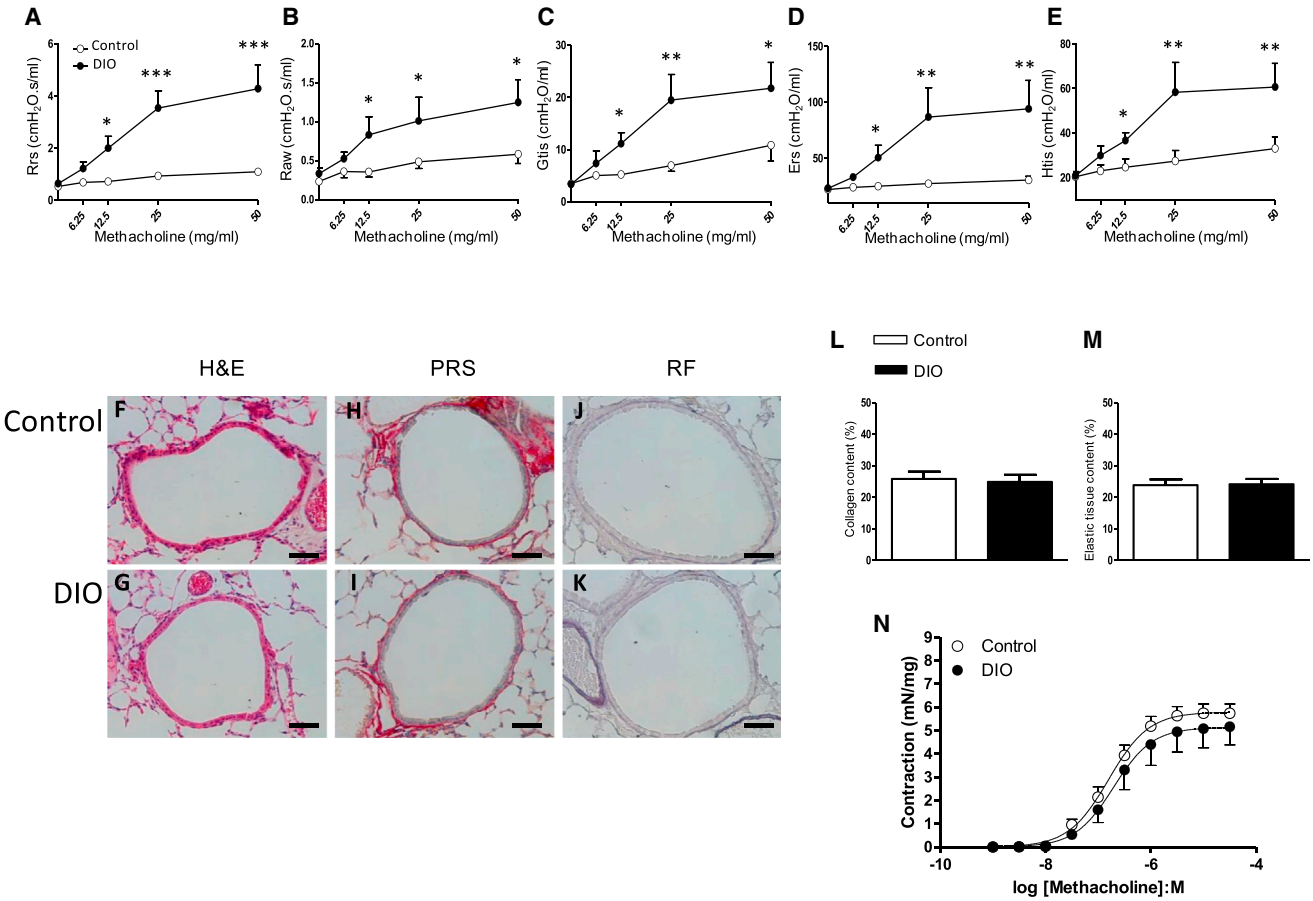

Figure 1. HFD-Induced Obesity Produces AHR in Mice

(A–E) Measurements of (A) Rrs, (B) Raw, (C) Gtis, (D) Ers, and (E) Htis in control and DIO groups are shown (*$p < 0.05$, **$p < 0.01$, ***$p < 0.001$ compared to control group; n = 8).

(F–K) Representative images of histology for the lungs from DIO and control groups stained with (F and G) H&E, (H and I) picrosirius red staining (PRS), and (J and K) oxidized resorcin fuchsin (ORF) are shown.

(L and M) Quantifications of (L) collagen and (M) elastic tissue contents are shown (scale bars, 100 μm; n = 8).

(N) Concentration-response curves to methacholine in isolated bronchial rings from both DIO and control groups are shown (n = 6). All data are expressed as mean ± SEM.

See also Figure S1.

The direct actions of insulin on metabolic tissues are crucial for whole-body metabolic homeostasis. However, several central insulin actions also have been recognized to control important aspects of glucose and fat metabolism (Brüning et al., 2000; Koch et al., 2008; Myers and Olson, 2012; Rother et al., 2012). Endogenous insulin crosses the blood-brain barrier through a saturable, insulin receptor (IR)-mediated process in brain capillary endothelial cells (Baura et al., 1993; Calhau et al., 2002), thus explaining the strong correlations between CNS and peripheral insulin levels found in different animal species (Begg et al., 2013). This is consistent with the increased insulin levels at the brain in fasted obese rats (Begg et al., 2013). Insulin also regulates a number of systemic functions via activation of the parasympathetic pre-ganglionic nerves at the dorsal vagal complex (DVC), which comprises the DMV, nucleus tract solitary (NTS), and area postrema (AP) (Filippi et al., 2012). Although the IR is widely expressed at NA, DMV (Havrankova et al., 1978; Unger et al., 1991; Werther et al., 1987), and cholinergic nerves (Wang et al., 2009), the central regulatory actions of insulin through these nuclei on bronchial reactivity remain unknown. Given the abundance of airway-related cholinergic nerves in the central areas and the increased ACh levels in the lungs of high-fat diet (HFD) obese mice (Arteaga-Solis et al., 2013), we aimed to investigate the modulation of cholinergic output into the airways by central insulin via ARPF activation and its implication for the pathogenesis of obesity-related asthma. We show here that intracerebroventricular (ICV)-injected insulin increases mice airway reactivity and that ICV insulin immunoneutralization restores airway reactivity in hyperinsulinemic obese mice. The insulin-induced AHR in obese mice is secondary to the stimulation of ERK signaling at ARPFs located at the DMV and NA, which convey parasympathetic outflow to the lungs.

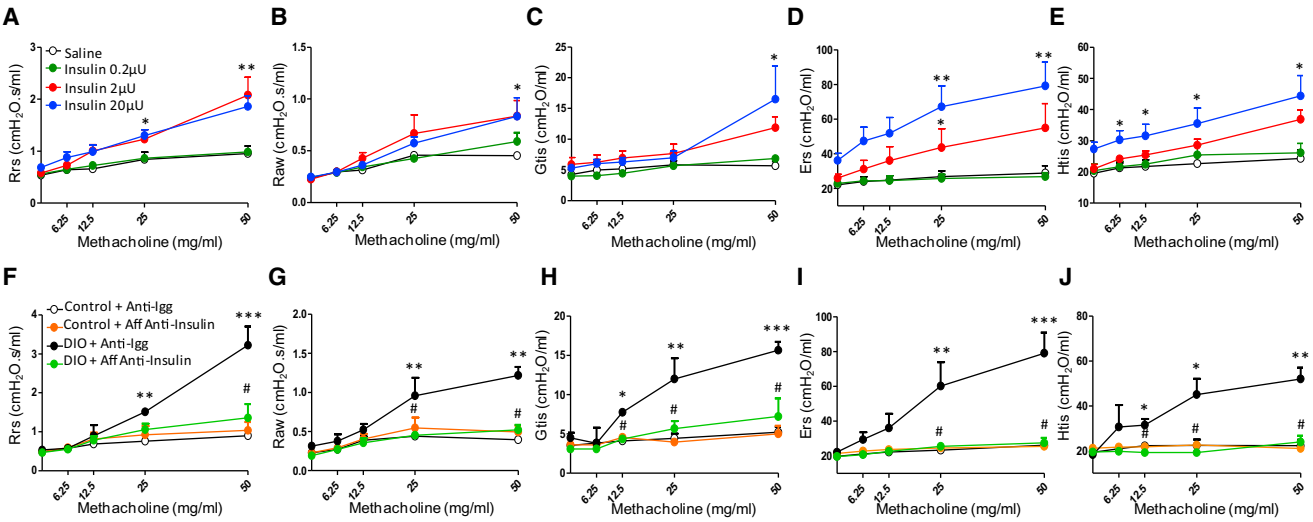

Figure 2. Central Hyperinsulinemia Causes AHR in Mice

(A–E) Measurements of (A) Rrs, (B) Raw, (C) Gtis, (D) Ers, and (E) Htis 30 min after ICV microinjection of saline or insulin at 0.2, 2, or 20 μU in C57BL6/J wild-type (WT) mice are shown (*$p < 0.05$, **$p < 0.01$ compared to group injected with saline; n = 7).

(F–J) Measurements of (F) Rrs, (G) Raw, (H) Gtis, (I) Ers, and (J) Htis in control and DIO groups microinjected via ICV with either anti-Igg or Affibody anti-insulin are shown (*$p < 0.05$, **$p < 0.01$, ***$p < 0.001$ compared to control + Anti-Igg group; #$p < 0.05$ when comparing DIO + Affibody anti-insulin group with DIO + anti-Igg group; n = 5).

See also Figure S2.

RESULTS

High-Fat-Fed Obese Mice Exhibit AHR Regardless of Inflammatory Cell Infiltration

Four-weeks aging C57BL6/J male mice were made obese by feeding a high-fat diet during 12 weeks. At the end of this period, mice developed obesity and presented hyperinsulinemia (Figures S1A–S1D), insulin resistance, and glucose intolerance (Figures S1E–S1H). Although there are some controversies related to insulin levels in CNS after a high-fat diet, these discrepancies seems to be related to the animal model used, but in fasted high-fat-fed obese rodents there are remarkable increases in fasted insulin levels in the brain (2-fold increase), which correlate with serum insulin levels (Begg et al., 2013). We further evaluated the pulmonary mechanics of control and diet-induced obese (DIO) mice by measuring airways resistance (Raw), resistance of the respiratory system (Rrs), tissue resistance (Gtis), elastance of the respiratory system (Ers), and tissue elastance (Htis). Methacholine produced a significant increase in airway reactivity in both groups (Figures 1A–1E; Figures S2I–S2M). However, all the mechanical parameters were significantly greater in DIO mice (Figures 1A–1E), which is in accordance with previous studies (Arteaga Solis et al., 2013; Johnston et al., 2008).

Histological evaluation in lungs of both groups revealed neither lung infiltration by inflammatory cells (Figures 1F and 1G) nor airway remodeling, as evaluated by measuring collagen and elastic tissue contents by pycrosirius and oxidized resorcin-fuchsin staining, respectively (Figures 1H–1M). In accordance, the number of total inflammatory cells, eosinophils, mast cells, and neutrophils in the bronchoalveolar lavage fluid (BALF) did not differ between control and DIO groups (Figures S1N–S1Q), confirming that innate AHR in our animal model does not rely on inflammatory cell infiltration. We further moved on to investigate whether the increase in airway responsiveness was due to local bronchial hyperreactivity. For this purpose, we performed concentration-response curves to methacholine (0.001–100 μM) in isolated bronchus rings isolated from lean and DIO mice. No changes in the bronchial smooth muscle contractile responses between lean and DIO mice were found (Figure 1N), indicating that in vivo AHR is not secondary to local hypercontractility.

High Levels of Central Insulin Produce AHR by Activating Cholinergic Nerves

Besides increased plasma glucose levels, obese/insulin-resistant subjects usually present a compensatory hyperinsulinemia, which may lead to plenty of secondary complications, such as cancer, cardiovascular diseases, and benign prostatic hyperplasia (Contreras et al., 2010; Heuson et al., 1972; Heuson and Legros, 1972; Vikram et al., 2010). At the level of the CNS, insulin regulates food intake, body weight, reproduction, and adiposity along with other peripheral functions, such as gastric motility (Blake and Smith, 2012; Brown et al., 2006; Brüning et al., 2000; Koch et al., 2008). As we did not detect changes in local bronchial reactivity, tissue remodeling, and inflammatory status in DIO mice, we hypothesized that elevated levels of insulin in the CNS lead to an increased cholinergic output into the airways causing an exacerbated bronchoconstriction in these animals.

Therefore, we next moved to assess whether ICV-delivered insulin increases the pulmonary mechanics in both control and DIO mice. In control mice, we found that insulin injected 30 min before the pulmonary mechanics measurements significantly

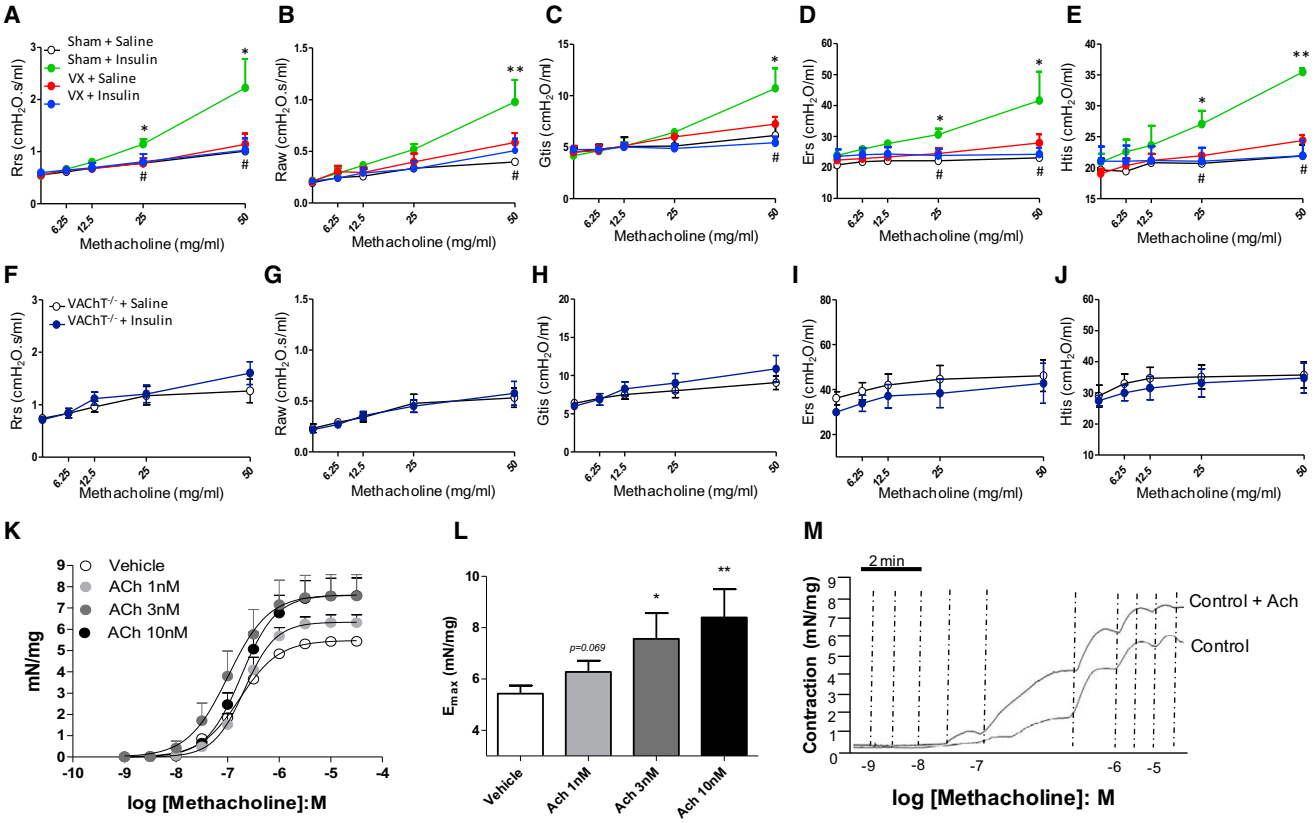

Figure 3. Central Insulin Potentiates Methacholine-Induced Bronchoconstriction through the Activation of Cholinergic Neurons

(A–E) Measurements of (A) Rrs, (B) Raw, (C) Gtis, (D) Ers, and (E) Htis, assessed in sham and VX mice, 30 min after ICV microinjection of either saline or insulin (2 μU) are shown (*$p < 0.05$, **$p < 0.01$ compared to sham + saline group; #$p < 0.05$ when comparing VX + insulin with sham + insulin groups; n = 5).

(F–J) Measurements of (F) Rrs, (G) Raw, (H) Gtis, (I) Ers, and (J) Htis in VAChT KD$^{HOM-/-}$ mice microinjected via ICV with either saline or insulin (2 μU) 30 min prior to the experiment are shown (n = 4–5).

(K) Concentration-response curves to methacholine in the absence or presence of pre-incubated ACh (1, 3, and 10 nM) in bronchial rings from control mice are shown.

(L) Maximal responses (E_{max}) to methacoline in the absence and presence of pre-incubated ACh (1, 3, and 10 nM) are shown.

(M) Representative traces of the contractions induced by methacholine in the absence or presence of pre-incubated ACh are shown (*$p < 0.05$, **$p < 0.01$ compared to non-treated bronchial rings). All data are expressed as mean ± SEM.

See also Figure S3.

increased Rrs, Raw, Gtis, Ers, and Htis, at concentrations of 2 and 20 μU ($p < 0.05$) (Figures 2A–2E), indicating that centrally injected insulin is capable of potentiating bronchoconstriction in response to inhaled methacholine. We also measured serum insulin levels 30 min after ICV insulin microinjection, but found no changes either in serum insulin (0.44 ± 0.1 and 0.37 ± 0.1 ng/ml before and after ICV insulin injection, respectively; n = 5) nor in plasma glucose (141.0 ± 1.4 and 146.8 ± 3.0 mg/dl before and after ICV insulin injection, respectively; n = 5) compared to basal levels (Figures S2A and S2B), confirming that insulin-induced increases in mechanical parameters in control mice are not a consequence of the peripheral actions of insulin. As opposed to control mice, ICV-injected insulin did not produce any changes in AHR in DIO mice (Figures S2C–S2G), probably due to local insulin resistance. However, upon immunoneutralization of central insulin by using an Affibody anti-insulin ICV, applied 30 min before mechanical measurements, we detected a full restoration of the airway reactivity of DIO mice with no changes in control mice (Figures 2F–2J). ICV injection of Affibody anti-insulin did not change blood glucose levels (Figures S2H and S2I).

To evaluate whether central insulin effects were mediated through the activation of a cholinergic innervation, we first performed ICV insulin injection in bilateral cervical vagotomized (VX) control mice. ICV-injected insulin produced consistent bronchoconstriction in the sham group, while it failed to induce AHR in the VX group (Figures 3A–3E). Bilateral vagotomy also normalized airway reactivity in response to methacholine in DIO mice (Figures S3A–S3E). Next, we used vesicle ACh transporter (VAChT) knockdown mice (VAChT KD$^{HOM-/-}$), which have an approximately 70% reduction in the release of ACh (Prado et al., 2006), to evaluate the bronchial reactivity. Insulin failed to increase methacholine-induced bronchoconstriction in VAChT KD$^{HOM-/-}$ mice (Figures 3F–3J), while it produced a full

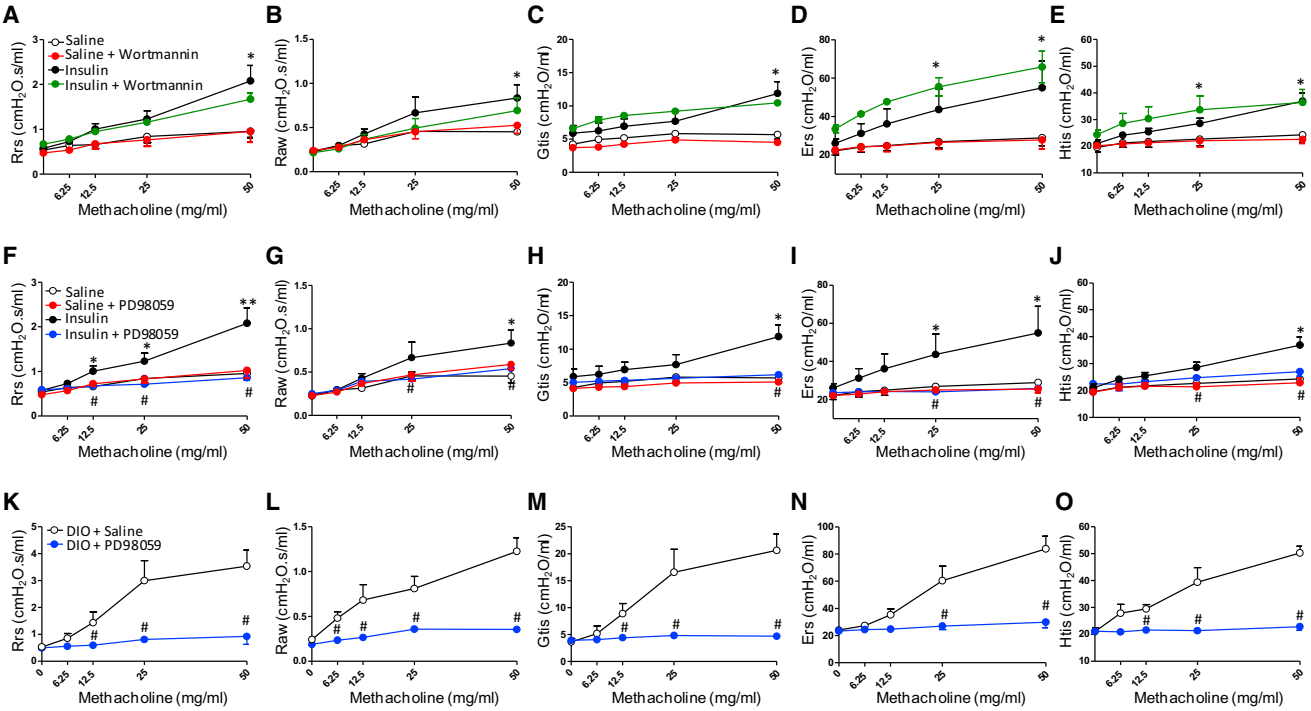

Figure 4. ERK, but not PI3K, Inhibitor Protects Mice against Insulin-Induced AHR

(A–E) Measurements of (A) Rrs, (B) Raw, (C) Gtis, (D) Ers, and (E) Htis 30 min after ICV microinjection of insulin (2 μU) in the presence or absence of PI3K inhibitor wortmannin (30 nM) in C57BL6/J WT mice are shown (*$p < 0.05$ compared to group injected with saline).

(F–J) Comparisons of all pulmonary mechanical parameters 30 min after ICV microinjection of insulin (2 μU) in the presence or absence of MEK/ERK inhibitor PD98059 (100 μM) in C57BL6/J WT mice are shown (*$p < 0.05$ compared to group injected with saline; #$p < 0.05$ when comparing insulin + PD98059 group with insulin group).

(K–O) Assessments of pulmonary mechanics in DIO mice microinjected via ICV with either saline or PD98059 (100 μM) 30 min prior to the experiment are shown. Data are expressed as mean ± SEM (n = 5–7; #$p < 0.01$ compared to DIO + saline group).

bronchoconstriction in the correspondent C57BL6/N3 background mice (Figures S3F–S3J).

As we did not observe a significant increase in the basal airway reactivity in either obese mice or control mice stimulated with insulin, we further aimed to assess whether a concentration of ACh that is not able to increase the bronchial reactivity per se can potentiate the methacholine-induced dose-response contractions in ex vivo preparations of bronchial rings mounted in organ baths. We first tested different ACh concentrations (1, 3, 10, and 30 nM), and found that only 30 nM was capable of directly producing bronchial contraction (data not shown, n = 4). We next performed concentration-response curves to methacholine in the absence or presence of pre-incubated ACh at the concentrations that were unable to produce bronchoconstriction (1, 3, and 10 nM). We found that methacholine-induced contractions were significantly potentiated by ACh at 3 nM ($p < 0.05$) and 10 nM ($p < 0.01$), whereas a trend to increase was observed with 1 nM ($p = 0.069$) pre-incubated ACh (Figures 3K–3M), suggesting that even low concentrations of ACh, which are unable to induce brochoconstriction per se, are capable of potentiating methacholine-induced bronchoconstriction. These data explain why both obesity-associated central hyperinsulinemia and centrally applied insulin potentiate in vivo bronchial contractile responses to methacholine in a cholinergic-dependent manner, without changing basal lung tone. We also performed concentration-response curves to methacholine in the presence of pre-incubated ACh in obese mice. We found that ACh potentiated contractile responses to methacholine in the DIO group to the same extent as in the control group (Figures S3K and S3L), indicating that bronchus from DIO mice is not more sensitive to ACh than the controls, once more proving that local bronchial hypersensitivity to cholinergic agonists does not drive AHR in obese mice.

ICV Insulin Induces Bronchoconstriction by Activating ERK in the CNS

IRs and downstream PI3K/AKT and MAPK signaling effectors are all expressed throughout the brain (Filippi et al., 2012; Folli et al., 1994; Pardini et al., 2006). Insulin microinjection into the DVC activates ERK1/2, triggering a signaling cascade to lower hepatic glucose production (Filippi et al., 2012). With these concepts in mind, we tested the hypothesis that central actions of insulin were due to stimulation of the ERK1/2 pathway in cholinergic nerves. We first performed insulin ICV injections in the presence and absence of either the PI3K inhibitor wortmannin (30 nM) or the ERK inhibitor PD98059 (100 μM), after which lung mechanical parameters were evaluated. In control (lean) mice, wortmannin failed to reduce insulin-induced bronchoconstriction (Figures 4A–4E), whereas PD98059 prevented central

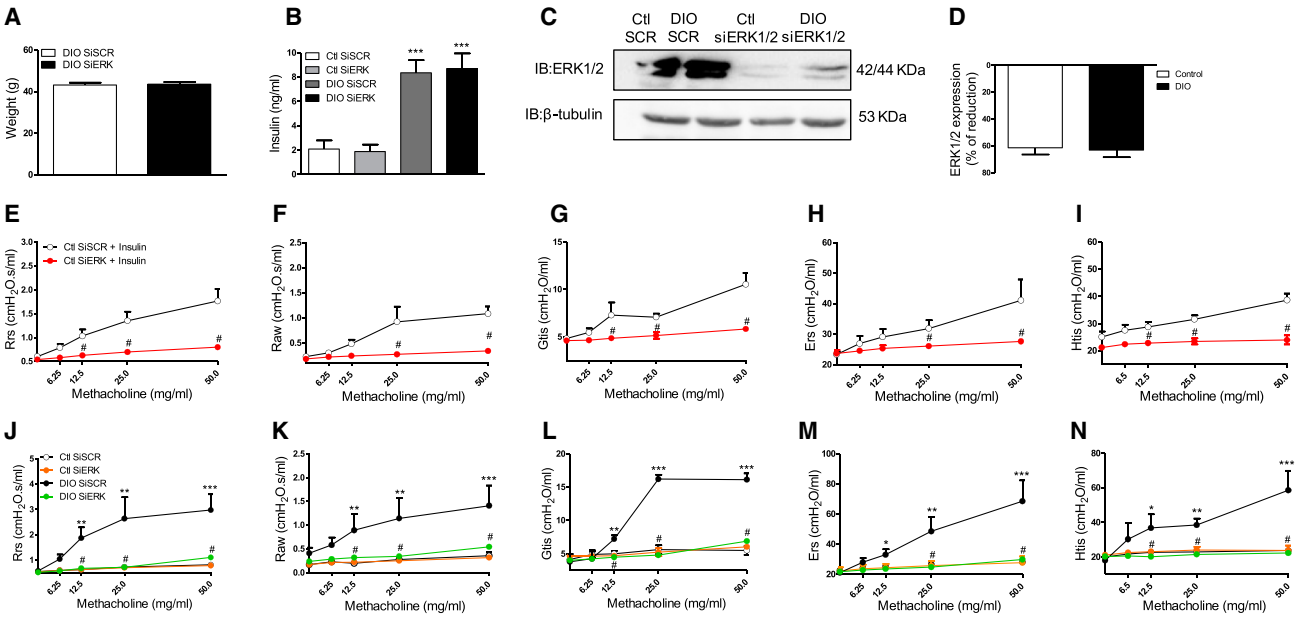

Figure 5. Insulin-Induced AHR Occurs via ERK Pathway Activation

(A and B) (A) Body weight and (B) plasma insulin levels in control and DIO mice intracerebroventricularly treated with siSCR or siERK1/2 are shown (n = 5).

(C and D) Representative (C) blots and (D) bar graphs expressing in percentage (%) of reduction of ERK1/2 protein expression in the brain stem from control and DIO mice intracerebroventricularly treated with siERK1/2 are shown (n = 5).

(E–I) Measurements of (E) Rrs, (F) Raw, (G) Gtis, (H) Ers, and (I) Htis 30 min after ICV microinjection of insulin (2 μU) in siSCR and siERK groups are shown (#$p < 0.01$ compared to siSCR + insulin group; n = 5).

(J–N) Assessments of pulmonary mechanics in control siSCR, control siERK, DIO siSCR, and DIO siERK groups are shown (*$p < 0.05$, **$p < 0.01$, ***$p < 0.001$ compared to control siSCR; # $p < 0.05$ when comparing DIO siERK with DIO siSCR group [two-way ANOVA]). All data are expressed as mean ± SEM (n = 5–7).

insulin-induced AHR (Figures 4F–4J). In DIO mice, microinjections of PD98059 also fully restored the airways' response (Figures 4K–4O). ICV injection of PD98059 did not modify blood glucose levels (Figures S4A and S4B).

To confirm these data, we treated obese and control mice with either a small interfering RNA (siRNA) for ERK1 and 2 (siERK1/2) or the scrambled siRNA (siSCR) via ICV during 3 days prior to lung mechanical evaluation. Obese mice did not change body weight and serum insulin levels (Figures 5A and 5B), and the reduction of ERK1/2 expression achieved in the brain stem of both control and DIO mice was around 60% (Figures 5C and 5D). Insulin elevated AHR in the siSCR group, but failed to produce AHR in siERK1/2 mice (Figures 5E–5I). AHR was increased in the DIO siSCR group, whereas siERK1/2 normalized all the alterations of the pulmonary mechanics (Figures 5J–5N).

Central Hyperinsulinemia Activates the ERK-Signaling Pathway in Cholinergic Neurons Situated on the DMV and NA

Next, we evaluated insulin signal transduction in airway-related nuclei that projects parasympathetic nerves into the lung. For this purpose, we assessed IR and ERK1/2 phosphorylation under basal and insulin-stimulated conditions through immunofluorescence. ICV-injected insulin produced a phosphorylation of IR (p-IRβ) and ERK1/2 (p-ERK1/2) in the DMV and rNA (Figures 6A–6D). Moreover, both p-IRβ and p-ERK1/2 co-localized with choline acetyltransferase (ChAT) staining, a well-known marker of cholinergic nerves (Figures 6A–6D), reinforcing that insulin activates cholinergic nerves at both the DMV and NA via the ERK/1/2 pathway, thus producing AHR.

As our images revealed that DMV and NA were responsive to insulin stimulation, we next separately dissect the DVC and the ventral bulb (VB), which are the regions where the DMV and NA are located, respectively, to explore the insulin-signaling pathway under basal and insulin-stimulated conditions. While ICV-injected insulin produced p-IRβ, phosphorylation of AKT (p-AKT), and p-ERK in the control group at both the DMV and NA, it did not change phosphorylation levels of these proteins in the DIO group (Figures 7A–7F). On the other hand, basal IR, AKT, and ERK phosphorylation were higher in DIO mice compared to control mice (Figures 7A–7F).

DISCUSSION

There appears to be at least two distinct asthma phenotypes of obese patients: (1) those with early-onset asthma and high serum IgE (T_H2-high) and (2) those with late-onset asthma and low serum IgE (T_H2-low). The incidence of this last phenotype highlighted the possibility that non-T_H2 components are likely to co-regulate airway dynamics under pathological conditions, and that the pathophysiology of obesity-related asthma might involve both non-T_H2 and endocrine pathways. In fact, a non-T_H2 but also inflammatory phenotype, involving innate immunity rather than adaptive immunity, has been described as a

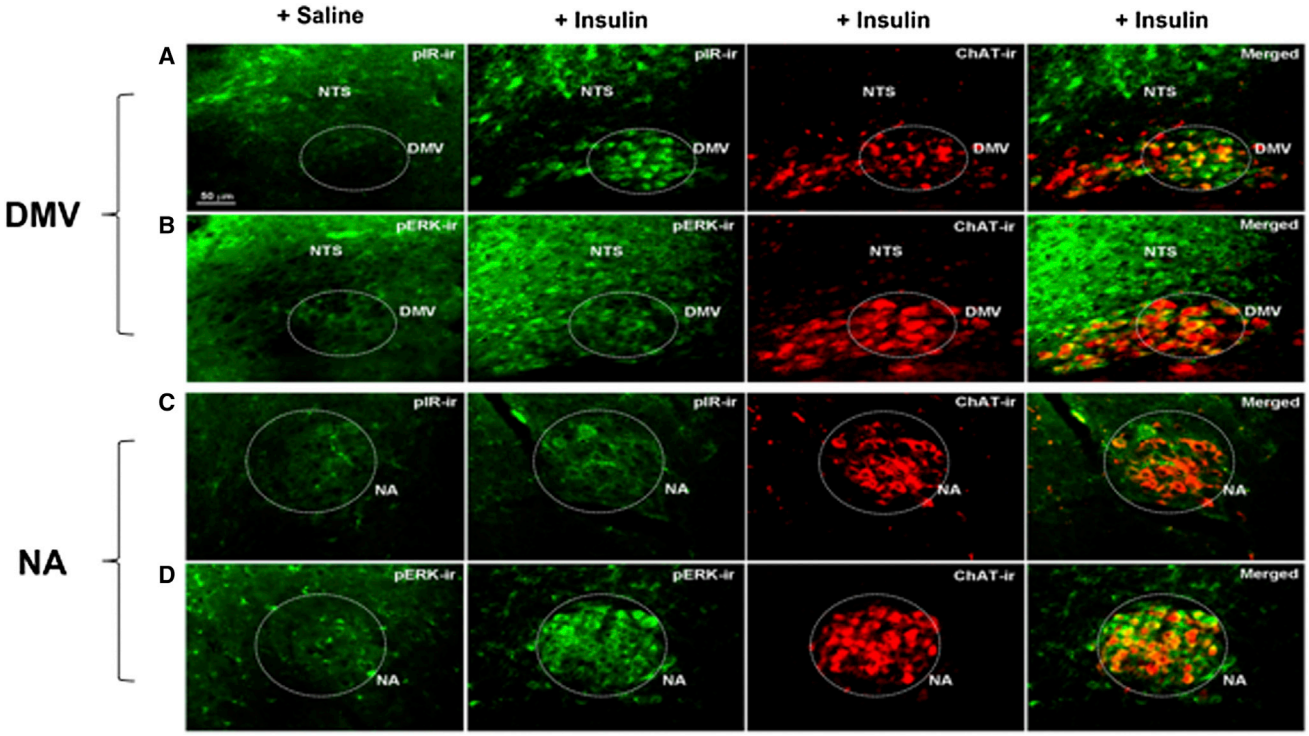

Figure 6. Insulin Promotes Phosphorylation of IR and ERK in Cholinergic Neurons Located at the NA and DMV

(A) Immunofluorescence shows p-IRβ, ChAT, and merge in the DMV of mice microinjected with either saline or insulin (2 μU) via ICV 10 min prior to dissection (n = 4).

(B) Immunofluorescence shows p-ERK, ChAT, and merge in the DMV (n = 4).

(C) Immunofluorescence shows p-IRβ, ChAT, and merge in the NA (n = 4).

(D) Immunofluorescence shows p-ERK, ChAT, and merge in the NA (n = 4).

component facilitating AHR in obesity (Kim et al., 2014; Kasahara et al., 2014). On the other hand, an inflammation-independent neuroendocrine system is capable of regulating airway tone and participating in the pathogenesis of obesity-related asthma phenotype. In the present study, we added an important concept regarding the neuroendocrine regulation of the airway reactivity in obesity by demonstrating that either central hyperinsulinemia secondary to obesity or ICV-injected insulin is able to increase AHR by stimulating ARPFs at the DMV and NA via the ERK pathway. Moreover, our data show an increase in all lung mechanical parameters in response to ICV-injected insulin, including Gtis and Htis, indicating that central insulin is capable of modulating not only the more calibrous bronchial branches, but also the responsiveness of the very distal bronchioles and lung tissue. Notwithstanding, small diameter airways are known to be richly innervated by cholinergic fibers, which are the main mediators of airway contraction (Canning, 2006).

Although the direct delivery of insulin into the brain is potentially pharmacological, our demonstration that neutralization of centrally circulating insulin prevents the hyperinsulinemia-induced AHR in the DIO group highlights the relevance of insulin action at ARPFs in these animals. The mechanical pulmonary parameters did not change in normoinsulinemic control mice after insulin neutralization, confirming that excessive rather than physiological levels of serum insulin are responsible for ARPF-mediated AHR. In addition, regardless of the body weight of the animal, central hyperinsulinemia is capable of potentiating bronchoconstriction per se. Our findings are consistent with recent studies conducted in either humans or mice reporting that hyperinsulinemia can be regarded as an independent risk factor for AHR (Nie et al., 2014; Thuesen et al., 2009).

High-fat-fed obese mice were reported to have increased ACh levels in the lungs, indicating an increased parasympathetic activity in the lungs of these animas (Arteaga-Solis et al., 2013). In our study, we found that insulin effects on lung reactivity rely on cholinergic innervation, which is projected to the lungs through ARPFs. Accordingly, ICV-injected insulin failed to potentiate methacholine-induced bronchoconstriction in both VX and VAChT KD$^{HOM-/-}$ mice, indicating that central insulin produces AHR by activating pre-ganglionic cholinergic nerves, thus increasing cholinergic outflow into the lungs. Peripheral firing of autonomic cholinergic nerves may not be excluded as an additional mechanism facilitating AHR in obesity/hyperinsulinemic condition (Nie et al., 2014). However, we showed no increases in peripheral serum insulin after ICV injection of insulin, reinforcing that the herein-observed insulin effects were indeed a consequence of its central excitatory activity instead of its peripheral actions.

IR stimulation by insulin leads to the recruitment and phosphorylation of receptor substrates such as IRS and Shc proteins.

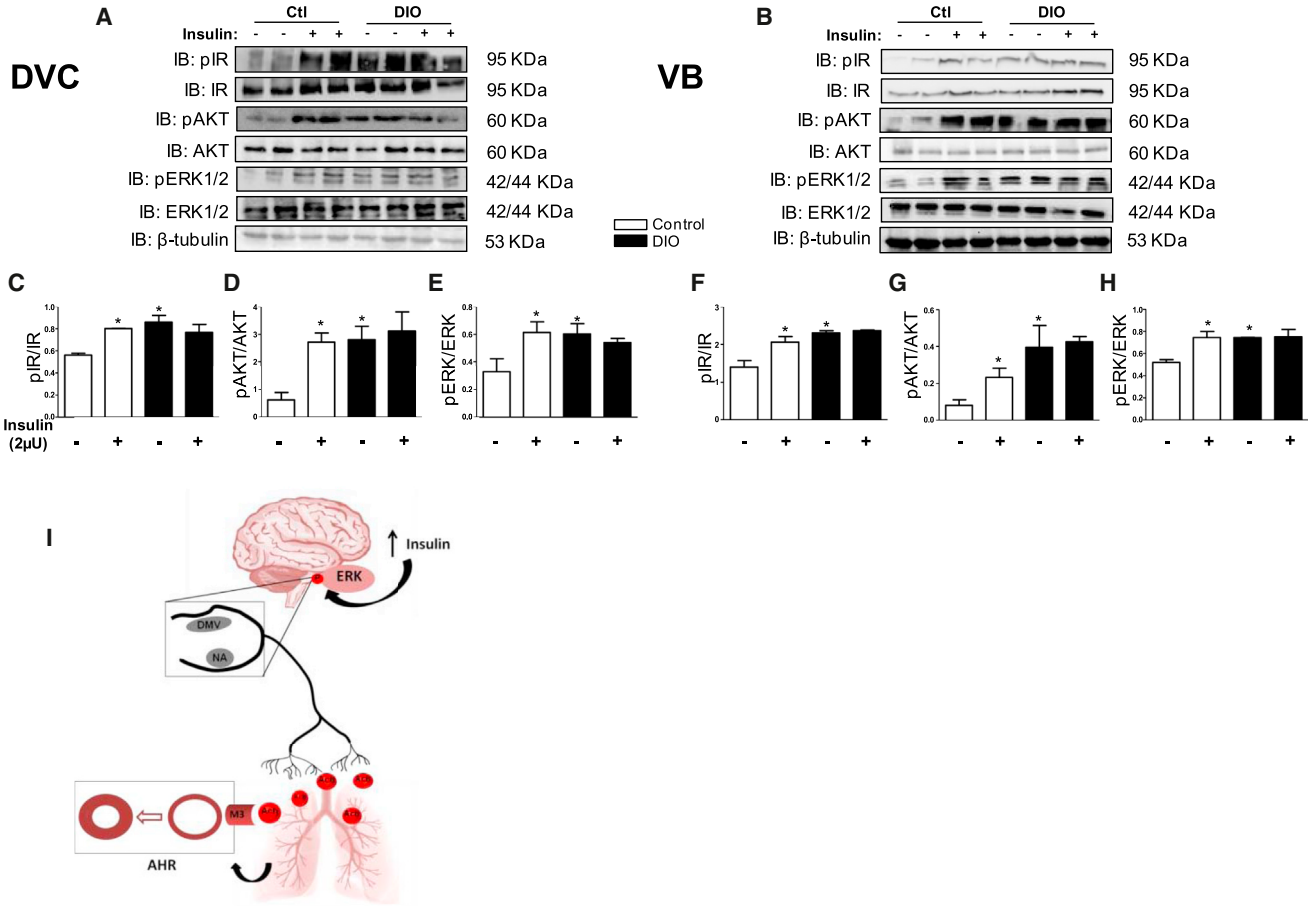

Figure 7. Central Hyperinsulinemia Increases Phosphorylation of IR and ERK in Airway-Related Pre-ganglionic Cholinergic Neurons

(A and C–E) Representative (A) blots and protein expression of (C) p-IRβ, (D) p-AKT, and (E) p-ERK in the DVC of control and DIO groups microinjected with saline or insulin (2 μU) via ICV 10 min prior to dissection are shown.

(B and F–H) Representative (B) blots and protein expression of (F) p-IRβ, (G) p-AKT, and (H) p-ERK in the VB of control and DIO groups microinjected with saline or insulin (2 μU) via ICV 10 min prior to dissection are shown. Data are expressed as mean ± SEM of 4–6 animals (*$p < 0.05$ compared to non-stimulated control group).

(I) Central insulin activates ERK-signaling pathway in the rNA and DMV at the brain stem, increasing ACh release into the lungs, thus producing AHR through the stimulation of M3 muscarinic receptors.

By one side, Shc activates the Ras-MAPK pathway, activating ERK1/2, whereas by the other side, IRS (1/2/3) proteins mostly activate the PI3K-Akt pathway by recruiting and activating PI3K, leading to the generation of second messenger PIP_3 (Kleinridders et al., 2014; Rask-Madsen and Kahn, 2012). Membrane-bound PIP_3 recruits and activates PDK-1, which phosphorylates and activates Akt. Our data suggest that insulin recruits ERK1/2 to activate cholinergic nerves instead of PI3K/Akt, as the centrally applied insulin failed to produce AHR when injected either in the presence of the ERK inhibitor PD98059 or in siERK1/2-treated mice, whereas the PI3K inhibitor wortmannin had no effect. Although we consistently showed the dependence of ERK activation for the central insulin-mediated AHR, we cannot neglect that inhibition/deletion of the ERK-signaling pathway in the brain stem also may blunt the shuttling of blood-borne insulin into the cerebrospinal fluid (CSF). Such ERK-dependent transport of circulating leptin into the CSF recently has been shown to be operated by tanycytes in the hypothalamus (Balland et al., 2014). Tanycyte-like cells are known to also reside in the AP, which lies next to the DVC (Langlet et al., 2013). Along with these genetic and pharmacological evidences, we have demonstrated that centrally applied insulin induces phosphorylation of IR and ERK in the cholinergic neurons located at the DMV and NA. ERK is overactivated by excessive insulin levels in the CNS of high-fat-fed obese rats (Filippi et al., 2012). Our results matches with this concept, as IR and ERK phosphorylation levels were upregulated at basal state in the obese group. Moreover, it is likely that the IR/ERK-signaling pathway was maximally activated in the brain stem of DIO mice, as it did not respond to additional insulin stimulation (Figures 4E–4L), explaining why additional ICV insulin infusion into already hyperinsulinemic DIO mice did not produce additional AHR.

Collectively, our findings indicate that central insulin activates the ERK pathway in cholinergic ARPFs, producing an increase

in parasympathetic outflow into the lungs and yielding AHR (Figure 4M). This study narrows down the effect of obesity and hyperinsulinemia on AHR via a specific signaling pathway in a discreet area of the brain. The presence of this non-T_H2 component in obesity-related asthma explains why most of obese subjects are resistant to glucocorticoid drug treatment. The present knowledge may drive new therapeutic strategies for the treatment of this peculiar asthma phenotype.

EXPERIMENTAL PROCEDURES

Animals

All animal procedures and experimental protocols were in accordance with the Ethical Principles in Animal Research adopted by the Brazilian College for Animal Experimentation (COBEA) and were approved by the institutional Committee for Ethics in Animal Research/State University of Campinas (CEEA-UNICAMP). C57BL6/J mice were used. Animals were fed for 12–14 weeks with either a standard chow or a high-fat diet to induce obesity. We also used vesicle ACh transporter (VAChT) homozygous knockdown mice (VAChT $KD^{HOM-/-}$) (Prado et al., 2006).

ICV Injections and Pulmonary Mechanics

Mice were previously anesthetized with a mix of ketamine and xylazin. After that, mice were stereotaxically instrumented (Stoelting Apparatus) to implant stainless steel 26G cannulas in the right lateral ventricle. The coordinates used from the bregma were: anterior/posterior, 0.4 mm; lateral, 0.8 mm; and dorso/ventral, 2.0 mm. After 5 days of recovery, mice were utilized for the pulmonary mechanics measurements.

For this purpose, we used the forced oscillation technique with a FlexiVent (SCIREQ). The mice were sedated with an intraperitoneal (i.p.) injection of tiopental (33 mg/kg). A tracheostomy was done with an 18G cannula, and the mouse was connected to the FlexiVent. The procedure was done in mice with closed chest. The mice were ventilated at 150 Hz, tidal volume (VT) 10 l/kg, and positive end-expiratory pressure (PEEP) level of 3 cmH_2O. In obese mice over 30 g, a VT of 0.3 ml was used to avoid hyperinflation of the lung due to VT calculated from their exaggerated body weights. Dose-response curves to inhaled methacholine chloride (Sigma) were done in increasing concentrations (6.25, 12.5, 25.0, and 50.0 mg/ml). The following mechanical parameters were evaluated: Rrs, Raw, Gtis, Ers, and Htis.

SUPPLEMENTAL INFORMATION

Supplemental Information includes Supplemental Experimental Procedures and four figures and can be found with this article online at http://dx.doi.org/10.1016/j.celrep.2015.04.012.

AUTHOR CONTRIBUTIONS

The experiments were carried out by L.O.S.L., F.M.A.-C., M.C.C., E.C.A., and R.F.M. in the laboratories of J.D., E.A., M.A.M., L.A.V., and M.J.A.S. C.M.P., M.A.P., and V.F.P. provided the VAChT KD^{HOM} mice and revised the manuscript. L.O.S.L., F.F., M.C.C., E.C.A., J.D., and M.J.A.S. collected, analyzed, and interpreted the data. L.O.S.L., J.D., E.A., M.A.M., and M.J.A.S. conceived and designed the experiments. L.O.S.L., F.F., E.A., L.A.V., and M.J.A.S. wrote the paper.

ACKNOWLEDGMENTS

We thank Andrey dos Santos, Dioze Guadagnini, and Sara Hamaguchi for the competent technical support. This study was supported by grants from Instituto Nacional de Ciência e Tecnologia (INCT) and Obesidade e Diabetes and Research, Innovation and Dissemination Centers (CEPID), which are supported by Conselho Nacional de Pesquisa (CNPq) and Fundação de Amparo à Pesquisa do Estado de São Paulo (FAPESP), respectively. L.O.S.L. was supported by a FAPESP post-doctoral fellowship.

Received: June 7, 2014
Revised: January 1, 2015
Accepted: April 3, 2015
Published: April 30, 2015

REFERENCES

Al-Alwan, A., Bates, J.H., Chapman, D.G., Kaminsky, D.A., DeSarno, M.J., Irvin, C.G., and Dixon, A.E. (2014). The nonallergic asthma of obesity. A matter of distal lung compliance. Am. J. Respir. Crit. Care Med. *189*, 1494–1502.

Arshi, M., Cardinal, J., Hill, R.J., Davies, P.S., and Wainwright, C. (2010). Asthma and insulin resistance in children. Respirology *15*, 779–784.

Arteaga-Solis, E., Zee, T., Emala, C.W., Vinson, C., Wess, J., and Karsenty, G. (2013). Inhibition of leptin regulation of parasympathetic signaling as a cause of extreme body weight-associated asthma. Cell Metab. *17*, 35–48.

Baker, D.G., McDonald, D.M., Basbaum, C.B., and Mitchell, R.A. (1986). The architecture of nerves and ganglia of the ferret trachea as revealed by acetylcholinesterase histochemistry. J. Comp. Neurol. *246*, 513–526.

Balland, E., Dam, J., Langlet, F., Caron, E., Steculorum, S., Messina, A., Rasika, S., Falluel-Morel, A., Anouar, Y., Dehouck, B., et al. (2014). Hypothalamic tanycytes are an ERK-gated conduit for leptin into the brain. Cell Metab. *19*, 293–301.

Baura, G.D., Foster, D.M., Porte, D., Jr., Kahn, S.E., Bergman, R.N., Cobelli, C., and Schwartz, M.W. (1993). Saturable transport of insulin from plasma into the central nervous system of dogs in vivo. A mechanism for regulated insulin delivery to the brain. J. Clin. Invest. *92*, 1824–1830.

Begg, D.P., Mul, J.D., Liu, M., Reedy, B.M., D'Alessio, D.A., Seeley, R.J., and Woods, S.C. (2013). Reversal of diet-induced obesity increases insulin transport into cerebrospinal fluid and restores sensitivity to the anorexic action of central insulin in male rats. Endocrinology *154*, 1047–1054.

Blake, C.B., and Smith, B.N. (2012). Insulin reduces excitation in gastric-related neurons of the dorsal motor nucleus of the vagus. Am. J. Physiol. Regul. Integr. Comp. Physiol. *303*, R807–R814.

Brown, L.M., Clegg, D.J., Benoit, S.C., and Woods, S.C. (2006). Intraventricular insulin and leptin reduce food intake and body weight in C57BL/6J mice. Physiol. Behav. *89*, 687–691.

Brüning, J.C., Gautam, D., Burks, D.J., Gillette, J., Schubert, M., Orban, P.C., Klein, R., Krone, W., Müller-Wieland, D., and Kahn, C.R. (2000). Role of brain insulin receptor in control of body weight and reproduction. Science *289*, 2122–2125.

Calhau, C., Martel, F., Pinheiro-Silva, S., Pinheiro, H., Soares-da-Silva, P., Hipólito-Reis, C., and Azevedo, I. (2002). Modulation of insulin transport in rat brain microvessel endothelial cells by an ecto-phosphatase activity. J. Cell. Biochem. *84*, 389–400.

Canning, B.J. (2006). Reflex regulation of airway smooth muscle tone. J. Appl. Physiol. *101*, 971–985.

Contreras, C., Sánchez, A., Martínez, P., Raposo, R., Climent, B., García-Sacristán, A., Benedito, S., and Prieto, D. (2010). Insulin resistance in penile arteries from a rat model of metabolic syndrome. Br. J. Pharmacol. *161*, 350–364.

Dey, R.D., Altemus, J.B., Rodd, A., Mayer, B., Said, S.I., and Coburn, R.F. (1996). Neurochemical characterization of intrinsic neurons in ferret tracheal plexus. Am. J. Respir. Cell Mol. Biol. *14*, 207–216.

Dixon, A.E., Pratley, R.E., Forgione, P.M., Kaminsky, D.A., Whittaker-Leclair, L.A., Griffes, L.A., Garudathri, J., Raymond, D., Poynter, M.E., Bunn, J.Y., and Irvin, C.G. (2011). Effects of obesity and bariatric surgery on airway hyperresponsiveness, asthma control, and inflammation. J. Allergy Clin. Immunol. *128*, 508–515.

Filippi, B.M., Yang, C.S., Tang, C., and Lam, T.K. (2012). Insulin activates Erk1/2 signaling in the dorsal vagal complex to inhibit glucose production. Cell Metab. *16*, 500–510.

Folli, F., Bonfanti, L., Renard, E., Kahn, C.R., and Merighi, A. (1994). Insulin receptor substrate-1 (IRS-1) distribution in the rat central nervous system. J. Neurosci. *14*, 6412–6422.

Fontán, J.J., Diec, C.T., and Velloff, C.R. (2000). Bilateral distribution of vagal motor and sensory nerve fibers in the rat's lungs and airways. Am. J. Physiol. Regul. Integr. Comp. Physiol. *279*, R713–R728.

Havrankova, J., Roth, J., and Brownstein, M. (1978). Insulin receptors are widely distributed in the central nervous system of the rat. Nature *272*, 827–829.

Heuson, J.C., and Legros, N. (1972). Influence of insulin deprivation on growth of the 7,12-dimethylbenz(a)anthracene-induced mammary carcinoma in rats subjected to alloxan diabetes and food restriction. Cancer Res. *32*, 226–232.

Heuson, J.C., Legros, N., and Heimann, R. (1972). Influence of insulin administration on growth of the 7,12-dimethylbenz(a)anthracene-induced mammary carcinoma in intact, oophorectomized, and hypophysectomized rats. Cancer Res. *32*, 233–238.

Husemoen, L.L., Glümer, C., Lau, C., Pisinger, C., Mørch, L.S., and Linneberg, A. (2008). Association of obesity and insulin resistance with asthma and aeroallergen sensitization. Allergy *63*, 575–582.

Johnston, R.A., Theman, T.A., Lu, F.L., Terry, R.D., Williams, E.S., and Shore, S.A. (2008). Diet-induced obesity causes innate airway hyperresponsiveness to methacholine and enhances ozone-induced pulmonary inflammation. J. Appl. Physiol. *104*, 1727–1735.

Kasahara, D.I., Kim, H.Y., Mathews, J.A., Verbout, N.G., Williams, A.S., Wurmbrand, A.P., Ninin, F.M., Neto, F.L., Benedito, L.A., Hug, C., et al. (2014). Pivotal role of IL-6 in the hyperinflammatory responses to subacute ozone in adiponectin-deficient mice. Am. J. Physiol. Lung Cell. Mol. Physiol. *306*, L508–L520.

Kim, H.Y., Lee, H.J., Chang, Y.J., Pichavant, M., Shore, S.A., Fitzgerald, K.A., Iwakura, Y., Israel, E., Bolger, K., Faul, J., et al. (2014). Interleukin-17-producing innate lymphoid cells and the NLRP3 inflammasome facilitate obesity-associated airway hyperreactivity. Nat. Med. *20*, 54–61.

Kleinridders, A., Ferris, H.A., Cai, W., and Kahn, C.R. (2014). Insulin action in brain regulates systemic metabolism and brain function. Diabetes *63*, 2232–2243.

Koch, L., Wunderlich, F.T., Seibler, J., Könner, A.C., Hampel, B., Irlenbusch, S., Brabant, G., Kahn, C.R., Schwenk, F., and Brüning, J.C. (2008). Central insulin action regulates peripheral glucose and fat metabolism in mice. J. Clin. Invest. *118*, 2132–2147.

Langlet, F., Mullier, A., Bouret, S.G., Prevot, V., and Dehouck, B. (2013). Tanycyte-like cells form a blood-cerebrospinal fluid barrier in the circumventricular organs of the mouse brain. J. Comp. Neurol. *521*, 3389–3405.

Leiria, L.O., Martins, M.A., and Saad, M.J. (2015). Obesity and asthma: beyond $T_{(H)}2$ inflammation. Metabolism *64*, 172–181.

Maize, D.F., Fedan, J.S., and Dey, R.D. (1998). Characterization of neural control and contractile function in airway smooth muscle of the ferret. Pulm. Pharmacol. Ther. *11*, 57–64.

Myers, M.G., Jr., and Olson, D.P. (2012). Central nervous system control of metabolism. Nature *491*, 357–363.

Nie, Z., Jacoby, D.B., and Fryer, A.D. (2014). Hyperinsulinemia potentiates airway responsiveness to parasympathetic nerve stimulation in obese rats. Am. J. Respir. Cell Mol. Biol. *51*, 251–261.

Pardini, A.W., Nguyen, H.T., Figlewicz, D.P., Baskin, D.G., Williams, D.L., Kim, F., and Schwartz, M.W. (2006). Distribution of insulin receptor substrate-2 in brain areas involved in energy homeostasis. Brain Res. *1112*, 169–178.

Pérez Fontán, J.J., and Velloff, C.R. (2001). Labeling of vagal motoneurons and central afferents after injection of cholera toxin B into the airway lumen. Am. J. Physiol. Lung Cell. Mol. Physiol. *280*, L152–L164.

Peters-Golden, M., Swern, A., Bird, S.S., Hustad, C.M., Grant, E., and Edelman, J.M. (2006). Influence of body mass index on the response to asthma controller agents. Eur. Respir. J. *27*, 495–503.

Prado, V.F., Martins-Silva, C., de Castro, B.M., Lima, R.F., Barros, D.M., Amaral, E., Ramsey, A.J., Sotnikova, T.D., Ramirez, M.R., Kim, H.G., et al. (2006). Mice deficient for the vesicular acetylcholine transporter are myasthenic and have deficits in object and social recognition. Neuron *51*, 601–612.

Rask-Madsen, C., and Kahn, C.R. (2012). Tissue-specific insulin signaling, metabolic syndrome, and cardiovascular disease. Arterioscler. Thromb. Vasc. Biol. *32*, 2052–2059.

Rother, E., Belgardt, B.F., Tsaousidou, E., Hampel, B., Waisman, A., Myers, M.G., Jr., and Brüning, J.C. (2012). Acute selective ablation of rat insulin promoter-expressing (RIPHER) neurons defines their orexigenic nature. Proc. Natl. Acad. Sci. USA *109*, 18132–18137.

Sideleva, O., Suratt, B.T., Black, K.E., Tharp, W.G., Pratley, R.E., Forgione, P., Dienz, O., Irvin, C.G., and Dixon, A.E. (2012). Obesity and asthma: an inflammatory disease of adipose tissue not the airway. Am. J. Respir. Crit. Care Med. *186*, 598–605.

Thuesen, B.H., Husemoen, L.L., Hersoug, L.G., Pisinger, C., and Linneberg, A. (2009). Insulin resistance as a predictor of incident asthma-like symptoms in adults. Clin. Exp. Allergy *39*, 700–707.

Unger, J.W., Moss, A.M., and Livingston, J.N. (1991). Immunohistochemical localization of insulin receptors and phosphotyrosine in the brainstem of the adult rat. Neuroscience *42*, 853–861.

Vikram, A., Jena, G.B., and Ramarao, P. (2010). Increased cell proliferation and contractility of prostate in insulin resistant rats: linking hyperinsulinemia with benign prostate hyperplasia. Prostate *70*, 79–89.

Wang, H., Wang, R., Zhao, Z., Ji, Z., Xu, S., Holscher, C., and Sheng, S. (2009). Coexistences of insulin signaling-related proteins and choline acetyltransferase in neurons. Brain Res. *1249*, 237–243.

Wenzel, S.E. (2012). Asthma phenotypes: the evolution from clinical to molecular approaches. Nat. Med. *18*, 716–725.

Werther, G.A., Hogg, A., Oldfield, B.J., McKinley, M.J., Figdor, R., Allen, A.M., and Mendelsohn, F.A. (1987). Localization and characterization of insulin receptors in rat brain and pituitary gland using in vitro autoradiography and computerized densitometry. Endocrinology *121*, 1562–1570.